CIRP Annals - Manufacturing Technology 74 (2025) 263–267

Contents lists available at ScienceDirect

CIRP Annals - Manufacturing Technology

journal homepage: https://www.editorialmanager.com/CIRP/default.aspx

# Improvement of anodic oxide film characteristics of Al-Cu alloy by refinement of IMCs with large-area electron beam irradiation

T. Shinonaga[a,*], A. Sebe[b], M. Taniguchi[c], T. Fujii[c], A. Okada (1)[a]

[a] Faculty of Environmental, Life, Natural Science & Technology, Okayama University, Okayama 7008530, Japan
[b] Graduate School of Environmental, Life, Natural Science & Technology, Okayama University, Okayama 7008530, Japan
[c] Shimano Research Laboratories, R&D Strategy Dept., SHIMANO INC., Osaka 5908577, Japan

ARTICLE INFO

*Article history:*
Available online 25 April 2025

*Keywords:*
Electron beam
aluminum
anodic oxide film

ABSTRACT

Al-Cu alloy has been widely applied to automobile products due to its light weight and high strength, but pitting corrosion easily occurs due to intermetallic compounds (IMCs) in Al-Cu alloy. Anodizing process has been conventionally performed to improve the corrosion resistance of Al-Cu alloy surface. However, IMCs in Al-Cu alloy lead to defects in anodic oxide film. In this study, refinement of IMCs in Al-Cu alloy surface by large-area EB irradiation was proposed. Experimental results show that reflectance and corrosion resistance of anodic oxide film formed on Al-Cu alloy surface are improved by refinement of IMCs with the EB irradiation.



## 1. Introduction

Al-Cu alloy has been widely applied to automobile and bicycle products due to its light weight and high strength. However, pitting corrosion easily occurs due to intermetallic compounds (IMCs) which are composed of elements such as Cu, Si and Mn in the Al-Cu alloy [1], since the IMCs act as a cathode in the Al matrix.

Corrosion resistance of Al alloy was improved by the coating method [2], but coated layer would be peeled from the surface. Anodizing process has been conventionally performed to improve corrosion resistance of Al-Cu alloy surface. Aluminum oxide film (anodic oxide film) with high corrosion resistance can be formed on the Al-Cu alloy surface by anodizing process. However, it was reported that IMCs are hardly oxidized during anodizing process, and IMCs lead to surface defects in the anodic oxide film [3]. As a result, anodic oxide film characteristics such as reflectance and corrosion resistance would deteriorate [4].

On the other hand, large-area electron beam (EB) of 60 mm in diameter can instantly and uniformly melt metal surface [5–6]. *Re*-solidified layer with fine microstructure is formed on the surface by the EB irradiation, and surface characteristics such as water repellency, corrosion resistance can be improved [7]. Shinonaga et al. [8] revealed that Mo-rich layer was uniformly formed on maraging steel surface by the EB irradiation. Mo element remains on maraging steel surface by the EB irradiation, but other elements were preferentially removed and/or melted, since boiling point and thermal conductivity of other elements are lower than those of Mo element. Therefore, it is highly expected that the IMCs in the Al-Cu alloy surface will be melted and refined by the EB irradiation, and surface characteristics of anodic oxide film formed on the Al-Cu alloy surface with EB irradiation will be improved.

In this study, refinement of IMCs in Al-Cu alloy surface by large-area EB irradiation was experimentally investigated. Mechanism for the refinement of IMCs was discussed by unsteady heat conduction analysis. After anodizing process, reflectance and corrosion resistance of the anodic oxide film on the Al-Cu alloy with the refinement of IMCs were examined.

## 2. Experimental procedure

Al-Cu alloy, A2014 in JIS specification (Al-5.0wt %, Cu-1.0wt %, Si-0.2wt %, Fe-0.9wt %, Mn-0.9wt %, Mg-0.9wt %) was used as a workpiece. T6 heat treatment was applied to the Al-Cu alloy. Table 1 shows thermal and physical properties of the Al-Cu alloy. The size of workpiece was 25 × 25 × 2 mm. Surface roughness of the Al-Cu alloy was set to 0.3 µm Rz or less by a mirror polishing.

Fig. 1 shows the schematic of experimental procedure in this experiment. First, the possibility of refinement of IMCs in Al-Cu alloy surface by the EB irradiation was examined. Table 2 shows EB conditions. Energy density $E_d$ of EB was fixed to 3.0 J/cm$^2$ and number of EB irradiation $N$ was varied from 1 to 10 shots.

Next, the mirror polished surface and the EB irradiated surface were anodized, respectively. Anodizing of Al-Cu alloy was performed by using a sulfuric acid method under free sulfuric acid with concentration of 220 ml/l, bath temperature of 293 K, and constant current electrolysis of 1.3 A/dm$^2$ for 10 min.

**Table 1**
Thermal and physical properties of Al-Cu alloy (A2014)

| | | | |
|---|---|---|---|
| Melting point | $\theta_m$ | [K] | 780 |
| Specific heat | $c$ | [J/(kg·K)] | 880 |
| Thermal conductivity | $\lambda$ | [W/(m·K)] | 150 |
| Density | $\rho$ | [g/cm$^3$] | 2.80 |

* Corresponding author.
*E-mail address:* shinonaga@okayama-u.ac.jp (T. Shinonaga).

https://doi.org/10.1016/j.cirp.2025.04.008

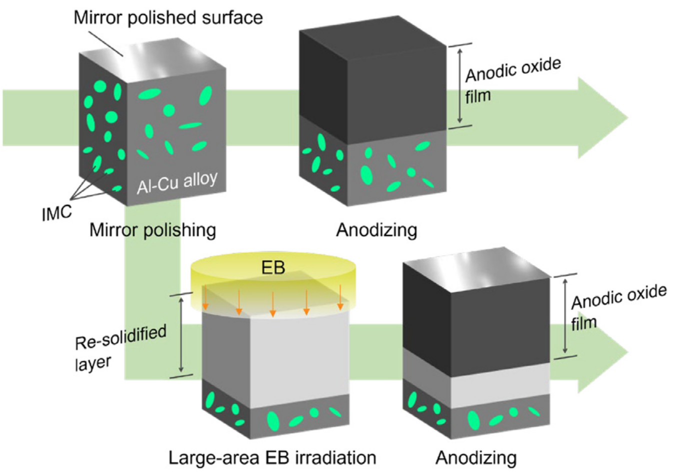


**Fig. 1.** Experimental procedure for mirror polishing, large-area EB irradiation, and anodizing.

**Table 2**
Large-area EB conditions

| | | | |
|---|---|---|---|
| Energy density | $E_d$ | [J/cm$^2$] | 3.0 |
| Number of irradiation | $N$ | [shot] | 1–10 |
| Pulse duration | $D_p$ | [$\mu$s] | 2.0 |
| Pulse frequency | $F_p$ | [Hz] | 0.125 |

The distributions of IMCs in the Al-Cu alloy surface before and after EB irradiation were examined by an energy dispersive X-ray spectroscopy (EDX). The anodic oxide film surface was observed by an optical microscope. Reflectance of film was measured using a microscope spectrometer. The reflectance $R$ was calculated by $R = R_r / R_d$, where $R_d$ is the amount of light directly measured from the light source, and $R_r$ is the amount of reflected light on the workpiece. The measurement area was 20 µm × 20 µm, and the reflectance was measured in the visible light range.

The copper accelerated salt spray (CASS) test was conducted to evaluate the corrosion resistance of anodic oxide film. In the CASS test, aqueous solution with copper chloride and sodium chloride was sprayed on the film surface. The corrosion resistance was evaluated by the number of pits and pitting depth on the film.

## 3. Refinement of intermetallic compounds by EB irradiation

Fig. 2 shows elemental mapping analysis results on the Al-Cu alloy surface before and after the EB irradiation. IMCs of Cu, Si and Mn with the size of 1–10 µm are partially distributed before the EB irradiation. On the other hand, after the EB irradiation at 5 shots, the IMCs on the surface are almost uniformly distributed, but some IMCs remains. After 10 shots, the size of IMCs becomes very fine, and the distribution is absolutely uniform. In addition, atomic percent of Cu, Si and Mn is almost same before and after the EB irradiation. These results suggest that IMCs are completely refined into the Al matrix without change of chemical composition by the EB irradiation.

In order to confirm the refinement of IMCs after the EB irradiation, crystal structures of Al-Cu alloy surface before and after EB irradiation were evaluated by X-ray diffraction (XRD). Fig. 3 shows XRD spectra of Al-Cu alloy surface. Before EB irradiation, there are some peaks of IMCs which consist of Cu, Mn, Mg and Si. After the EB irradiation, the peaks of IMCs are hardly confirmed. These results indicate that IMCs are completely refined into the Al matrix by the EB irradiation.

Fig. 4 shows cross-sectional images of Al-Cu alloy with and without EB irradiation. Re-solidified layer with fine microstructure is formed after 5 shots EB irradiation, but IMCs remain inside the re-solidified layer. In the case of 10 shots, re-solidified layer with a thickness of 12 µm is formed, and sufficient refinement of IMCs in the re-solidified layer can be confirmed. The refinement of IMCs may be caused by the melting and re-solidification of the IMCs through a

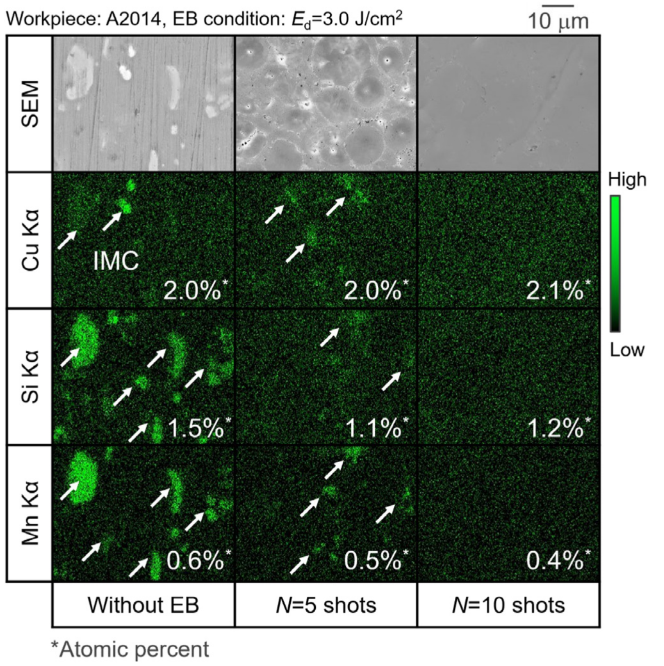


**Fig. 2.** Elemental mapping images of Al-Cu alloy surface before and after EB irradiation.

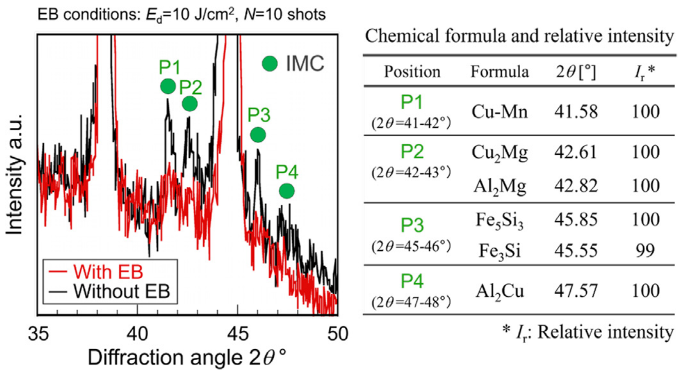


**Fig. 3.** XRD spectra of Al-Cu alloy surface before and after EB irradiation.

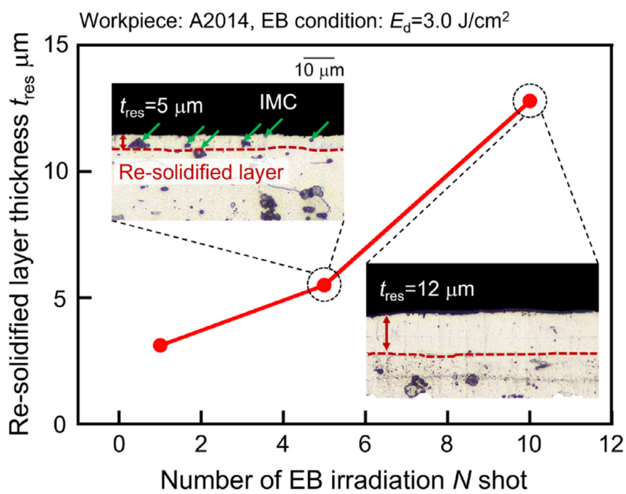


**Fig. 4.** Cross-sectional images of Al-Cu alloy and re-solidified layer thickness after EB irradiation.

rapid heating and cooling process during the EB irradiation. Fig. 4 also shows variation of resolidified layer thickness with number of EB irradiation. The resolidified layer thickness increased with the number of EB irradiation. After the EB irradiation at 10 shots, the re-solidified layer with refinement of IMCs is thicker than 5 µm, which is larger than thickness of anodic oxide film. Therefore, defect of anodic oxide film would be suppressed by formation of thicker re-solidified layer with refinement of IMCs.

## 4. Mechanism for refinement of IMC

Unsteady heat conduction analysis was conducted by using a commercial finite element method (FEM) program (ANSYS 17.0) to calculate the temperature history of Al-Cu alloy surface during EB irradiation. Fig. 5 shows the unsteady heat conduction analysis model. In the experiments, the workpiece was clamped with chucks made of stainless steel during the EB irradiation. Considering their symmetric shapes, rectangular FEM model of one cross-sectional shape of workpiece and chuck was built.

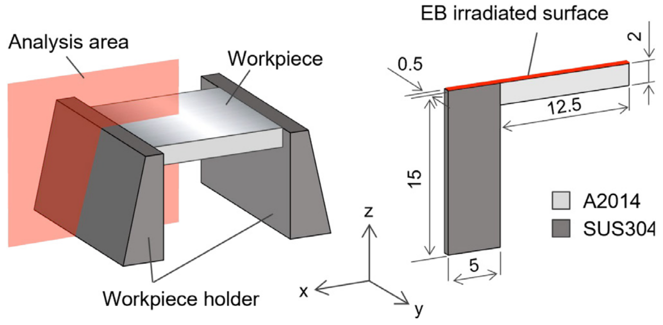


**Fig. 5.** Unsteady heat conduction analysis model.

Analysis conditions are shown in Table 3. In the analysis, only heat transfer between the workpiece and chuck was considered, since it is known that heat transfer by convection of gas can be neglected under the pressure $<10^{-2}$ Pa. In addition, latent heat of Al-Cu alloy was considered. Thermal and physical properties of Al-Cu alloy as shown in Table 1 was used. A heat energy input with considering the waveform of cathode voltage in pulse duration of 2.0 µs was applied to the workpiece and chuck surfaces, since the EB was irradiated to the upper sides of workpiece and chuck.

**Table 3**
Analysis conditions

| | | | |
|---|---|---|---|
| Energy density | $E_d$ | [J/cm$^2$] | 3.0 |
| Number of irradiation | $N$ | [shot] | 1 |
| Heat transfer | $H$ | [W/(m$^2$·K)] | 0 |
| Emissivity | $\varepsilon$ | | 0.2 |
| Room temperature | $T_r$ | [K] | 300 |

Fig. 6 shows temporal change in temperature distributions of Al-Cu alloy in large-area EB irradiation under 3.0 J/cm$^2$ and 1 shot. Red area is the area where temperature is above the boiling point of Al-Cu alloy, and the yellow one is the area where temperature is between the melting point and boiling one. As shown in the figure, the temperature rapidly rises in 0.9 µs. At 0.9 µs, the maximum temperature of top surface becomes about 1200 K, which is higher than the melting point (780 K) but lower than the boiling point (2743 K). The analysis results show that IMCs and matrix of Al-Cu alloy can be melted by the EB irradiation.

Fig. 7(a) shows the temperature history of EB irradiated Al-Cu alloy surface in the range from 1 to $10^7$ µs. The time interval of each EB pulse is about $10^7$ µs. The surface temperature falls rapidly and it becomes room temperature at about $10^3$ µs. It is known that the alloy elements dissolve or precipitate by heat-treatment at a certain temperature and cooling rate. Cooling rate after the EB irradiation is sufficiently faster than the cooling rate of continuous cooling transformation curve. These results indicate that a part of IMCs can be dissolved into the matrix during the EB irradiation.

Fig. 7(b) shows expected mechanism of refinement of IMCs by EB irradiation. At first, Al-Cu alloy surface with IMCs is melted by rapidly

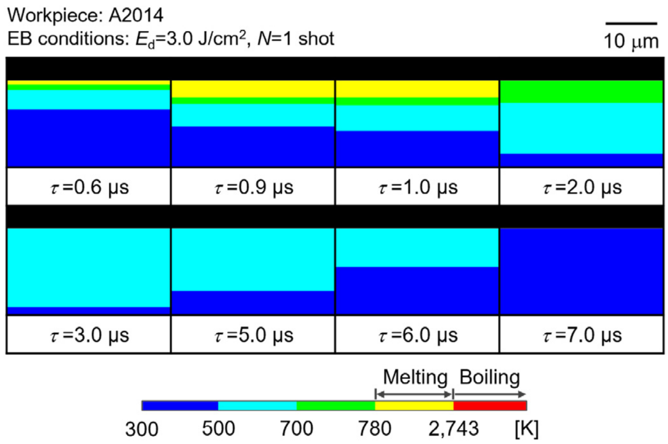


**Fig. 6.** Temporal change in temperature distributions of Al-Cu alloy in large-area EB irradiation.

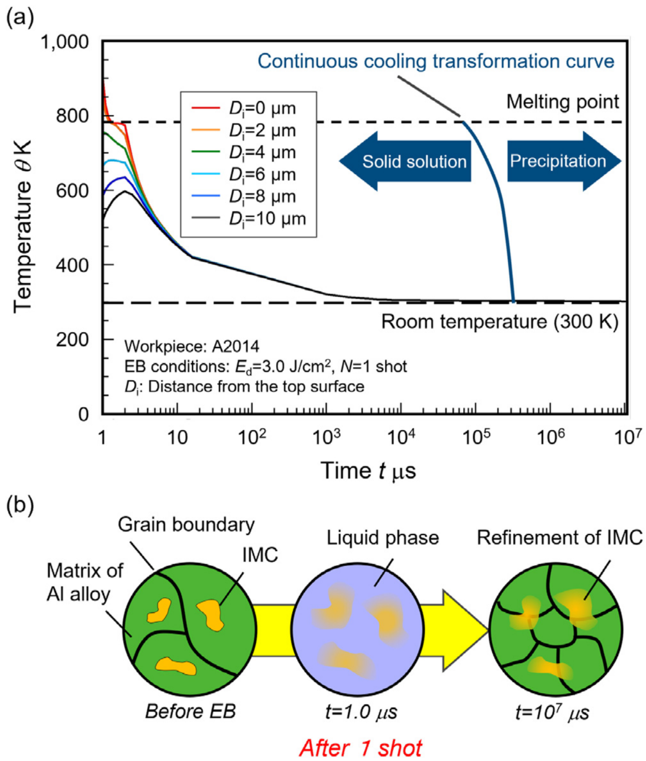


**Fig. 7.** (a) Temperature histories of EB irradiated Al-Cu alloy each distance from the top surface, and (b) expected mechanism of IMC refinement by EB irradiation.

heating with EB irradiation. Then, some IMCs are dissolved into the Al matrix. After that, some of IMCs and Al matrix become finer and dissolve when temperature rapidly drops after EB irradiation. By repeating this process, the IMCs are completely refined and dissolved into the Al-Cu alloy. The refinement of IMCs into Al-Cu alloy after the EB irradiation is confirmed from cross-sectional TEM images as shown in Fig. 8.

## 5. Anodic oxide film formation on al-cu alloy surface

Fig. 9 shows optical images of anodic oxide film surfaces which are formed on the Al-Cu alloy with and without EB irradiation. Cross-sectional TEM images of interface between the re-solidified layer and the anodic oxide film are also shown. The surface images show that many defects are generated on the anodic oxide film surface without the EB irradiation, while only a few defects are generated on the film surface with the EB irradiation. From TEM images, in the case without EB irradiation, anodic oxide film is formed from the base material which contains many IMCs. On the other hand, the film is formed from the re-solidified layer with refinement of IMCs after the EB

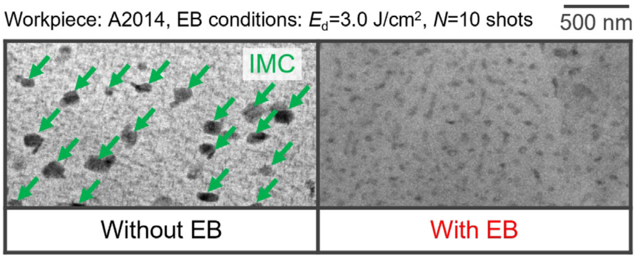


**Fig. 8.** Cross-sectional TEM images of Al-Cu alloy with and without EB irradiation.

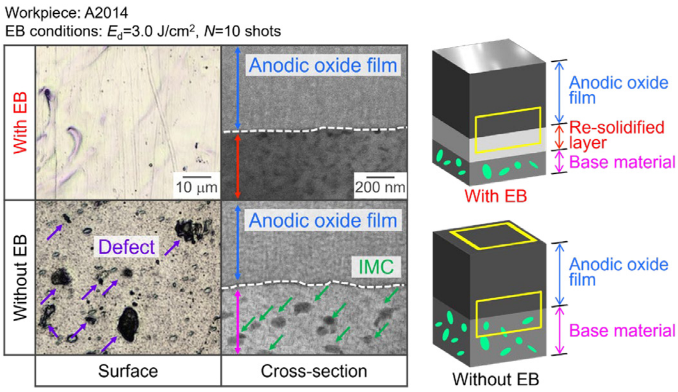


**Fig. 9.** Anodic oxide film surface and cross-sectional images formed on Al-Cu alloy with and without EB irradiation.

irradiation. Therefore, anodic oxide film with few defects can be successfully formed by the refinement of IMCs after the EB irradiation.

In the anodizing process, the anodized film grows by dissolution from the surface to a depth of several micrometer. Therefore, even if the surface is removed by mechanical polishing or milling at the nanometer scale, the surface characteristics of anodized film might not be improved since the IMCs remain at the micrometer scale in base metal. On the other hand, the large-area EB irradiation method can uniformly refine the IMCs to a depth of about 10 µm. Then, the surface characteristics of anodized film with EB irradiation might be improved. Large-area EB irradiation method is one of the useful surface treatments for refinement of IMCs.

## 6. Surface characteristics of anodic oxide film

Fig. 10 shows the reflectance of anodic oxide film surface formed on Al-Cu alloy with and without EB irradiation. Optical images of the film surfaces are also shown in the figure. The optical images show that the anodic oxide film on Al-Cu alloy with EB irradiation becomes brighter than that without EB irradiation. Reflectance of anodic oxide film surface on Al-Cu alloy with the EB irradiation is higher than that without EB irradiation in the visible light wavelength range. The reason for improvement of reflectance in the case of using the EB irradiation before anodizing is the refinement of IMCs composed of the Si and Mn in the Al-Cu alloy. Theses IMCs leads to generation of defects in the anodic oxide film surface, and the decrease of reflectance on the film surface.

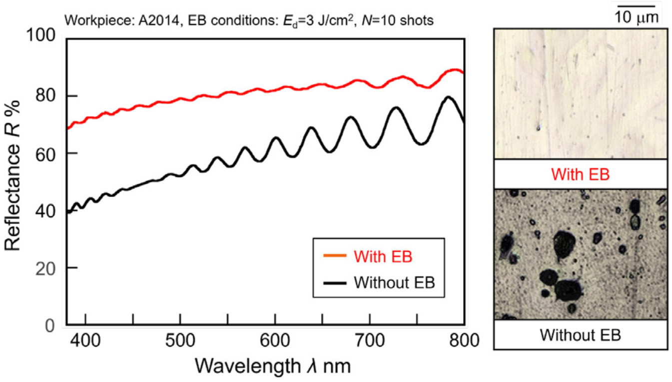


**Fig. 10.** Change in reflectance of anodic oxide film surfaces formed on Al-Cu alloy with and without EB irradiation.

Fig. 11 shows number of pits and pitting depth on anodic oxide film surfaces formed on the Al-Cu alloy with and without EB irradiation after corrosion test. Optical images of the film surfaces are also shown in the figure. Number of pits on the film surface formed on the Al-Cu alloy with the EB irradiation is reduced to one-third of that without EB irradiation. The reduction of pitting corrosion is also confirmed from the optical images. In addition, pitting depth of the film surface with the EB irradiation is much smaller than that without EB irradiation. Furthermore, pitting depth of the film without EB irradiation has large variation, but the pitting depth is less variation in the case with EB irradiation. Results in chapter 5 show that the anodic oxide film surface formed on Al-Cu alloy surface with the EB irradiation has a few defects due to refinement of IMCs in the Al-Cu alloy. Thus, the pitting corrosion hardly occurs on the film, and corrosion resistance is more improved.

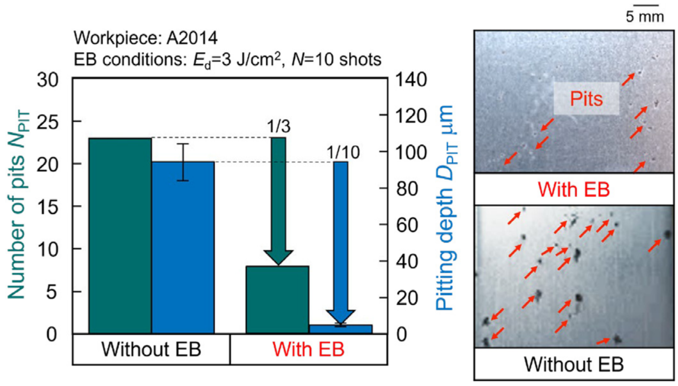


**Fig. 11.** Number of pits, pitting depth and optical images on anodic oxide film surfaces formed on Al-Cu alloy with and without EB irradiation.

## 7. Conclusions

In this study, refinement of IMCs in Al-Cu alloy surface by large-area EB irradiation was proposed. In addition, improvement of anodic oxide film characteristics by the refinement of IMCs with the EB irradiation was examined. Main conclusions obtained in this study are as follows,

1. Large-area EB irradiation enables refinement of IMCs in Al-Cu alloys surface without change of chemical composition, since temperature of EB irradiated surface rapidly rises above melting point of Al-Cu alloy, and the cooling rate is sufficiently faster.
2. Anodic oxide film formed on Al-Cu alloy surface with EB irradiation has less defects, and reflectance of the film becomes higher compared to that without EB irradiation.
3. Corrosion resistance of anodic oxide film formed on Al-Cu alloy surface with EB irradiation is more improved, since the number of pits and pitting depth reduce compared to those without EB irradiation.

### Declaration of competing interests

The authors declare that they have no known competing financial interests or personal relationships that could have appeared to influence the work reported in this paper.

### CRediT authorship contribution statement

**T. Shinonaga:** Writing – original draft, Visualization, Conceptualization. **A. Sebe:** Software, Investigation. **M. Taniguchi:** Methodology, Funding acquisition. **T. Fujii:** Resources, Data curation. **A. Okada:** Writing – review & editing, Supervision.

## References


[1] Chen GS, Gao M, Wei RP (1996) Microconstituent-induced pitting corrosion in aluminum alloy 2024-T3. *CORROSION* 52:8–15.

[2] Mahton Y, Kamde MA, Saha P (2024) Influence of Cu addition on the microstructure, and corrosion behavior of electroless Ni-Cu-P coating on squeeze-cast Al-Cu-Mg alloy. *Surface and Coatings Technology* 494:131544.

[3] Dasquet JP, Caillard D, Conforto E, Bonino JP, Bes R (2000) Investigation of the anodic oxide layer on 1050 and 2024T3 aluminium alloys by electron microscopy and electrochemical impedance spectroscopy. *Thin Solid Films* 37:183–190.

[4] Shimizu K, Brown GM, Habazaki H, Kobayashi K, Skeldon P, Thompson GE, Wood GC (2000) Selective oxidation of aluminium and interfacial enrichment of iron during anodic oxide growth on an Al6Fe phase. *Corros Sci* 42:831–840.

[5] Okada A, Kitada R, Okamoto Y, Uno Y (2011) Surface modification of cemented carbide by EB polishing. *CIRP Annals* 60:575–578.

[6] Shinonaga T, Yamaguchi A, Okamoto Y, Okada A (2021) Surface smoothing and repairing of additively manufactured metal products by large-area electron beam irradiation. *CIRP Annals* 70:143–146.

[7] Okada A, Okamoto Y, Uno Y, Uemura K (2014) Improvement of surface characteristics for long life of metal molds by large-area EB irradiation. *Journal of Materials Processing Technology* 214:1740–1748.

[8] Shinonaga T, Watanabe S, Yamaguchi A, Okada A (2023) Mo-rich layer formation on maraging steel and surface modification by large-area electron beam irradiation. *Journal of Materials Processing Technology* 311:117813.